Open Access Journal

Journal of Power Technologies 98 (4) (2018) 365–376

journal homepage:papers.itc.pw.edu.pl

The effect of various buffer battery maintenance regimes on the state of health of VRLA batteries

Piotr Ryś[a,*], Jacek Lipkowski[a], Maciej Siekierski[a], Piotr Biczel[b]

[a] *University of Technology Faculty of Chemistry, ul. Noakowskiego 3, 00-664 Warsaw, Poland;*
[b] *Warsaw University of Technology Faculty of Electrical Engineering, pl. Politechniki 1, 00-661 Warsaw, Poland*

Abstract

Modern society relies on the constant flow of quality electricity. Various safety measures in the form of uninterruptible power supplies (UPS) combined with diesel generation systems are used to ensure permanent power delivery to strategic services during a power outage. Batteries UPS systems are held in buffer mode to avoid the self discharge process progressing. The impact of various buffer battery maintenance regimes is an important factor in ensuring the reliability of UPS systems. A series of tests on five battery pairs were performed to estimate the impact of five different buffer regimes on the batteries' state of health. The tests were carried out in the span of one year, at heightened temperature to accelerate the negative impact of the said regimes on the batteries' state of health. The test results showed that, contrary to widely-accepted belief, rippling of the buffer charging current does not have a significant negative impact on battery health. A comparison did indeed show that rippled charging current delivered lower total capacity loss than unrippled current. Then desulfation was applied to the batteries after testing to estimate the amount of capacity that was lost due to sulfation. It determined that rippling promotes more irreversible capacity loss (not caused by sulfation) than unrippled current with the same average voltage. The insights gained from these tests could inform attempts by industry to slow down the deterioration of lead-acid batteries in UPS applications.

Keywords: Batteries; Lead-Acid; VRLA; State of Health; Buffering charge; Desulfation

1. Introduction

In the modern society there is a need for uninterrupted supply of electrical power. A whole raft of key systems at strategic locations such as power plants, communication centers, hospitals and military bases must be fully operational 24/7. Emergency diesel generators are ready to provide backup power should an outage occur. However, there is a time gap between the grid power cutting out and the generators achieving the minimum required power output. This delay has the potential to take down vital information technology systems, something that is to be avoided at all costs. Various systems have been designed and built to meet the need for an "uninterruptible power supply" (UPS). These backup units must produce sufficient power to sustain the key systems to which they are assigned. Lead-acid batteries are a perfect choice for UPS, as they have a flat discharge curve and are resistant to damage triggered by irregular discharge/charge cycles. Their cost per unit of capacity is also a positive factor in roles of this kind. The main general concern with lead-acid batteries is their power to weight ratio, but this is not a problem with stationary use, which is the norm for UPS batteries. Their maximum voltage per cell lies in the range of 2.2-2.3V, making it easy to string cells together for various applications. Maintenance-free or valve-regulated lead-acid (VRLA) battery designs are the preferred option for small uninterruptible power supplies, mostly because they offer a good service life and require little or no maintenance during their lifespan according to their manufacturers. For smaller systems, the VRLA design is most commonly used. Flooded batteries are common in large scale applications such as emergency lighting and emergency power systems and require maintenance in the form of monitoring electrolyte levels and replenishing the water that evaporates during normal battery operation [1, 2].

2. Theory

Reliability is paramount with UPS systems, particularly during their move from stand-by to activation, as their energy backup circuits must have an extremely low probability

*Corresponding author
Email address: prys@ch.pw.edu.pl (Piotr Ryś)

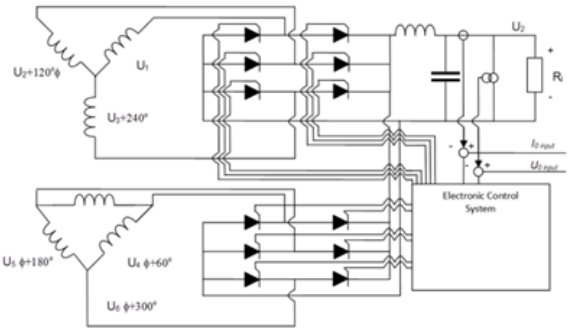

Figure 1: Simplified diagram of a thyristor based 12 pulse rectifier

of breakdown upon startup. Since lead-acid batteries form the basis for most of these systems, techniques are still being developed to predict the possible time of aging-related breakdown during operation. Various mathematical models [3, 4] have been designed based on different concepts to determine the aging of the battery and various estimates made for certain conditions.

2.1. Current rectification and its effect on batteries

A vital part of UPS design is the current rectifier, which operates in online system design as both battery charger and the circuit delivering power to the loads (either directly or through the inverter) or in offline design operates only as battery charger. Various arrays of semiconductor based elements can be used to achieve this goal [5]. Historically, the first rectifiers constructed were mechanical, but as time progressed they evolved into vacuum tube based designs and, later, rectifiers based on semiconductors such as diodes. To deliver the low-rippled rectification required for industrial applications and to ensure better control of system operation parameters, two main designs concepts have been developed: the thryristor and the transistor approach. While these two designs supply rectified current, the presence of rippling in the current poses an operational problem when charging batteries.

Thyristor based rectifiers are now used in appliances with power in the megawatt range. The thyristor based rectifier is depicted in diagram form in Fig. 1. In essence it is an extension of the concept of simple diode based rectifiers. The thyristor is triggered through the gate terminal, so a control unit can modify the parameters of the current supplied by either changing the phase angle of the currently triggering moment or delivering a selected number of semi-sine current pulses. The main drawback with using thyristor based rectifiers is the need to incorporate carefully adjusted filters into the design to limit the impact of voltage ripples to an acceptable level. This flaw increases their size and weight, thereby reducing their usability. It should also be noted that since thyristor based rectifiers have a negative impact on the power grid, causing AC current sine wave distortion, they require specially adjusted transformers.

The typical charging current generated by thyristor based rectifiers has a 12 pulse shaped ripple component overlaid over the direct current component. The generation of 12 pulse ripple is shown in schematic form in Fig. 2. The rippling component has a frequency of 600 Hz for the 12 pulse rectifier. The amplitude of the component is fairly large and can reach several dozen percent of the nominal current value. In some extreme circumstances values can be observed in excess of 100% of the mean value of the current's amperage. These extraordinary conditions can arise during the buffer charging of the battery. This type of charging current damages the battery, as it can lead to extensive gassing processes inside. This is a major problem characteristic mainly for the buffer charging of the battery, during which the actual current is small compared to the nominal current of the rectifier. The rectifier then works with a non-continuous current, which is particularly damaging to the battery. Consequently, the Eurobat standard [6] excludes the use of rectifiers of this type in charging VRLA batteries, as water replenishment is not available for them.

One rectifier design viewed as having far more potential is the pulse converter, which is transistor based [7]. As featured on Fig. 3 it has two important components: a 6 pulse diode based rectifier responsible for initial current rectification and a DC/DC converter that pitches the voltage value to the expected value and smoothes out the current output. The idea applied here is based on the use of fast-switching transistors within the DC/DC converter to further smooth out the rippling. Usually, these transistors are turned on and off with frequencies ranging from 10 to 50 kHz. A variable length triggering signal is delivered by the attached control unit. While the frequency remains a design feature of the rectifier, the momentary timespan of the pulse is adjusted on the basis of a comparison between the actual value of the voltage of the output capacitor and the expected reference value.

Compared to thyristor based rectifiers, pulse converters give a different spectrum of ripples---the rippling is sawtooth-like in nature, with frequency corresponding to the above mentioned switching one. Pulse converters are easily the most expensive solutions available on the market due to their complexity and component cost. They suffer from a drawback similar to that of thyristor based rectifiers, which cause the power grid to experience a significant amount of total harmonic distortions; similarly, they require specially adjusted transformers and filters to nullify this negative effect.

This class of rectifiers has to work with non-continuous current during the buffer charging. The shape of the charging current is close to non-contiguous triangular pulses, characterized by repetition frequency equal to that characterizing the signal switching of semiconductor valves. The discussion surrounding the impact on premature aging and damage to charged batteries originating from the presence of the rippling component of this kind is still unresolved [8, 9].

There is a dispute as to whether 12 pulse rectifier originated rippling is more damaging than high frequency sawtooth waves generated by pulse converters [5, 10, 11]. The complex nature of the aging processes occurring in the bat-

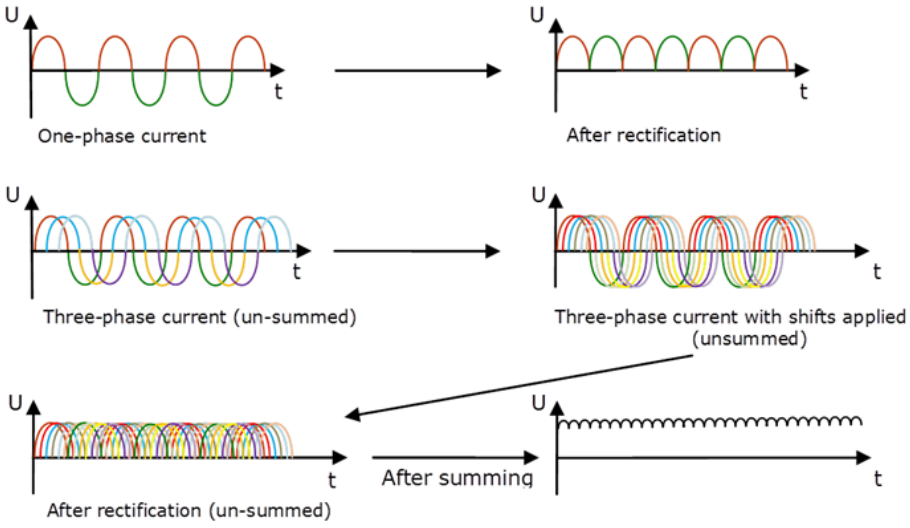

Figure 2: Creation of a 12 pulse ripple shape

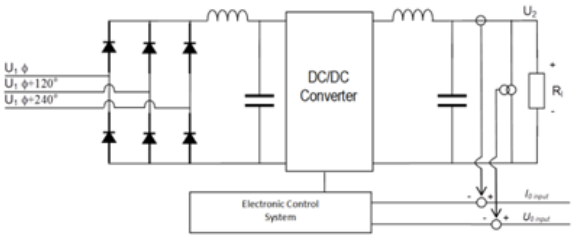

Figure 3: Simplified diagram of a pulse converter

teries means there is no clear-cut answer. Morever, the studies cited here relate predominately to work based on simulations. Commonly, though, rectifier manufacturers claim that pulse converters are less damaging to battery systems, while the system maintenance grounded electrical engineers tend to claim that 12 pulse rectifiers are neither worse nor better. Hence, it is reasonable to check whether these claims are true, by investigating capacity losses over time in lead-acid batteries buffered under various operation conditions---such as various types of rippling present in charging current, buffering voltages, temperatures and discharge currents.

2.2. Capacity losses in batteries

Under standard operating conditions, capacity loss is a very slow process. The speed of all aging processes is mostly dependent on both the internal temperature of the battery and the charging strategy applied, as well as the particular construction design of the cell. Since most UPS fitted batteries tend be stored in specially air conditioned rooms to keep temperature levels in check, the temperature impact is thought to be lessened. However, due to the enclosed design of some of the smaller UPS systems---which limits airflow---batteries can still suffer increased temperatures owing to the heat radiating from the electrical components of the system.

The only way to properly study battery properties during the deterioration process is through accelerated aging tests performed at higher temperatures. While there are some simulation techniques available that predict the rate of battery aging and the related capacity loss, they are neither universal nor fully reliable [12]. In some cases even the most elaborate models deliver inaccurate results. One of the troublesome conditions relates to the presence of rippled current, as most models treat the charging current as unrippled current. Moreover, even when applying higher temperatures to speed up the aging processes in the investigated battery, the typical testing regime still lasts in excess of one year.

It should be noted that the batteries themselves are large and the only way they can exchange heat is by convection, so they can age rapidly if thermal runaway occurs during operation. This serious problem can result in unexpected premature failure and hence temperature should be monitored during battery operation. Since temperature has such an impact on battery longevity, adjustments to the buffering voltage have to be made to ‘compensate’ for such conditions. This is referred to as “temperature compensation” and is based on an empirical equation where the voltage value to be added to or subtracted from the buffer voltage is calculated from the difference between the operating temperature and the reference temperature of 25°C (corresponding to the ‘perfect condition’). The formula for this is described in [1] and corresponds to lowering the buffer voltage by 3 mV per cell for each degree above 25°C.

2.3. Aging processes

Aging processes may be divided into those that are reversible and those that are irreversible. While capacity lost through reversible aging processes can be recovered by

through special charging techniques, irreversible processes pose a great problem in long term usage of batteries [1, 2].

Reversible aging processes mostly relate to sulfation: a process where crystals of $PbSO_4$ expand to the point of being quasi-inert in the reactions occurring during the charging process. The question of what exactly causes this change and what specific conditions promote sulfation are still for the most part unanswered, but it is widely recognized that undercharging batteries speeds up the process. It should be taken into account that excess sulfation can lead to irreversible mechanical damage to the structure of the active material through the formation of large crystals [2, 13, 14]. The other reversible process that can occur is acid stratification---non-uniform distribution of acid concentration in the battery---but this issue can be resolved mechanically by stirring or air-bubbling the acid solution. In VRLA batteries this process is:

1. current density distribution (not gravitation) driven, and
2. hard to counteract due to the gel state of the electrolyte making stirring impossible [2, 15].

'Gassing' is one of the irreversible aging processes, often referred to as water loss, which happens when a battery is charged with a voltage higher than the threshold beyond which water is decomposed into hydrogen and oxygen (2.3V per cell in ambient conditions). The voltage where this process occurs can be affected by the battery's construction or the chemical composition of the plates [16]. The problem with closed battery designs like VRLA and MF is that the water cannot be replenished, whereas flooded batteries usually have a removable cap so you can replenish the water and minimize the impact. This problem is alleviated by several design choices for VRLA and MF batteries. MF batteries can be fitted with catalytic caps, to regain some of the lost water from recombination of hydrogen and oxygen that escapes during operation. VRLA, a closed system, features a similar but more efficient catalyst, which enables excess gas to be recombined without it escaping from the battery [1, 2, 17, 18].

Another irreversible process is corrosion of the grid, which occurs on the positive plate. While chemical corrosion happening under the conditions present is a slow process, the aging process is accelerated through the existence of an electrochemical process. The aforementioned oxygen evolution that occurs on the positive plate causes in situ generation of atomic oxygen that causes much quicker corrosion and, in turn, electrical failure of the positive grid. The first sign of positive plate corrosion might be an increase in battery capacity, due to the lead grid being converted into lead oxide, which the battery can harness as an active material. This is not a beneficial effect, as the weakened lead grid suffers increased frailty, leading to a risk of mechanical failure [2].

One serious class of problems comes in the form of mechanical failures, which result from either aging processes or manufacturing faults. The nature of mechanical failures met in practical life includes: the shedding of some of the electrode active material, parts of the plate breaking off and internal connection failures caused by poor welding techniques. Another form of mechanical failure is swelling of the battery. This occurs due to an increase in volume of the material inside. Corrosion causes the lead that forms the grid to oxidize and since lead has a smaller volume than lead (IV) oxide by a ratio of 1:1.375 [19], the battery's volume increases as the corrosion progresses. As the battery ages, the corrosion can cause an increase in volume that may compromise the battery casing through mechanical stress from the lead products pressing against it [1, 2, 18].

2.4. Experiment Setup

All of the experiments which were conducted in this study were performed on ten new VRLA batteries, type LC-R121R3PU, manufactured by Panasonic. The batteries have a nominal capacity of 1.3 Ah and a nominal voltage of 12 V. All ten units originated from the same production lot. The batteries were grouped in five pairs and all experiments were doubled on two identical units to assure control of the reliability of the results. To speed up the process of battery deterioration, a heat-isolated oil bath was connected to the thermostat, to heat the batteries to 55°C; according to [2]this is the highest possible temperature that assures results corresponding to those obtained at the ambient temperature over a much longer timeframe. The batteries were connected to a custom-built junction box to facilitate the connecting of cables.

The voltages applied during float charging periods of the experiment were chosen to reflect research cited earlier in this paper. Two main goals were achieved through using the elevated temperature, namely the experiment was accelerated and the increased temperature enabled the authors to investigate the efficiency of temperature compensation in reducing the gassing processes occurring in the batteries.

The first battery pair was charged at a voltage of 13.8 V---the maximum charging trickle-use voltage mentioned in the battery's technical specifications.

The second battery pair was charged at a voltage of 13.35 V---which is the above mentioned charging voltage of the battery pair with overlaid temperature compensation for the 55°C present inside the oil bath. The buffer voltage was calculated using the formula provided earlier. Given that the batteries had six cells and the temperature in which the measurements were taking place was 55°C, the voltage needed to be substracted was calculated as 450 mV.

The third pair was purposefully sulfated through applying an undervoltage. This charge regime is characterized by applied voltage of 13V. This pair was set up as a reference to test the desulfation method described later in this section.

The fourth and fifth pairs were charged at the same voltage as the second pair, but a waveform was overlaid over the buffer charge voltage by means of a custom-built amplifier. For the fourth pair a wavefrom created through overlaying six half-sine waves of 180 mV amplitude and 600 Hz frequency (Fig. 4 Left) was used to simulate a thyristor based 12 pulse rectifier. For the fifth pair a sawtooth wave with amplitude of 67 mV and 15 kHz frequency (Fig. 4 Right),was

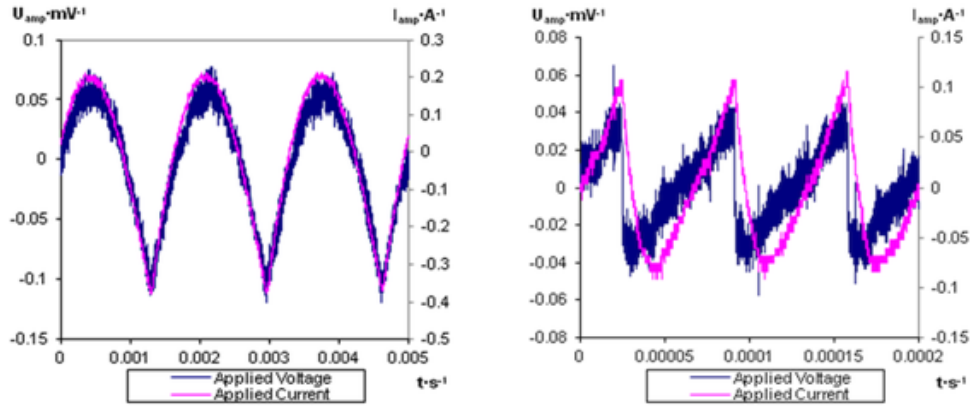

Figure 4: Oscillograms of the applied artificial rippling voltage signals and the corresponding current response of the cells stressed of left) 600Hz half-sine wave right) 15kHz sawtooth wave

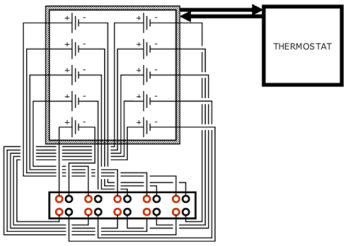

Figure 5: Diagram of connections between the junction box and batteries

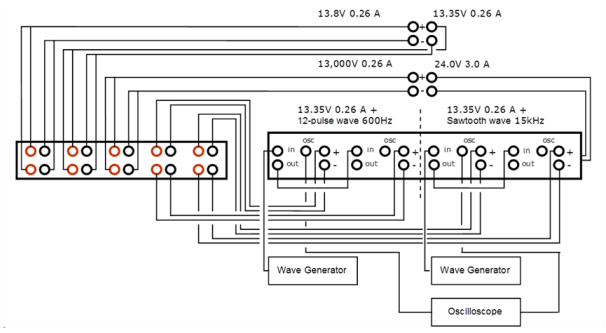

Figure 6: Diagram of connections between the junction box and the power supplies

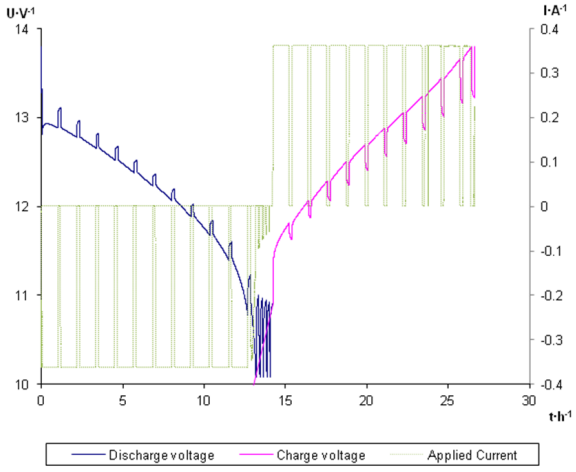

Figure 7: Exemplary current input and resulting voltage output of a battery in both discharge and charge sub-cycles

used to simulate a switching power supply board. A set of two BK Precision 9310 power supplies was used to provide well-controlled DC voltage resulting in a flow of ripple-free float-charging current during rest periods of battery pairs I, II and III. Three channels of a total four available were involved here, while the fourth was used to provide power to the custom-built amplifier that was delivering arbitrary formed voltage signals applied to force the flow of rippled float charge currents in the last two battery pairs. This custom-built four channel high current amplifier modulates the DC bias voltage with arbitrary waveforms supplied by external signal sources. A Tektronix Waveform Generator model AWG2021 was used to provide the simulated 12 pulse rectifier type and switching power supply type modulating signals. The voltage and current traces were monitored and gathered by a Tektronix 240D digital oscilloscope. Schematic diagrams of the connections between the batteries and the power supplies are shown in Fig. 5 and Fig. 6.

The measurement cycle consisted of subcycles of increasing discharge current interlaced with charging periods characterized by a constant charging rate equal to 130 mA (C/10). The successive discharge currents used in the following subcycles were: 130 mA (C/10), 260 mA (C/5), 430 mA (C/3), 650 mA (C/2) and 1300 mA (1C). The discharge phase of a cycle was considered finished when battery voltage of 10.08V was reached, while the charge phase was finished when battery voltage reached its designated level for the given battery. After the 1C subcycle completed, the new main cycle started with the C/10 regime. Battery cycling ended when a catastrophic failure of the battery pair was observed or after 9-10 full cycles (from C/10 to 1C). The exemplary current input and resulting voltage output of a battery in both the discharge and charge subcycles are presented in Fig. 7. The course of the entire experiment was estimated

for one year, including time taken for equipment maintenance and non-working periods (public holidays etc.).

For the purpose of the parallel polarization experiment a special discharge/charge algorithm was devised: for the subcycle during discharge the voltage was checked to see if it had reached 10.08V, if it had not reached 10.08V the discharge procedure proceeded until 130mAh of charge was spent. Then there was a period of 15 minutes where the OCV was measured. This procedure was repeated twelve times. Similarly, for the charge, the cell voltage was checked to see if it had reached a specified value in accordance with the pair's number, until 130mAh was delivered to the battery; followed if negative by the same period of OCV measurement as in the previous subcycle. This procedure was performed twelve times for the charge cycle as well. The full algorithm is presented in Fig. 8. The first discharge/charge cycle did not use this special algorithm to determine whether the batteries supplied were working correctly. These measurements were later used to calculate polarization resistance.

The capacity loss that occurred throughout the controlled discharge-charge cycles provides a good indication of how fast the battery wears out while remaining under a specific buffer regime. As a measure of deterioration, the discharge capacity values and data enabling estimation of polarization resistance were gathered in all the following cycles and compared after the experiment was completed and the appropriate estimations made.

The battery discharge experiments were performed using BioLogic's VMP-3 Electrochemical Workstation. The experimental setup delivered data that was used to describe the capacity changes and to determine the depth of deterioration of the internal battery structures, estimated through the increase in internal resistance values.

Calculation of polarization resistance values was based on Ohm's law:

$$\eta = 1 - \frac{1}{\varepsilon^{\kappa-1}} \tag{1}$$

where: U_{OCV} - open circuit voltage of the battery, U_{Load} - voltage of the battery under load, I - discharging/charging current.

Since it was not possible to properly measure U_{Load} in a direct manner, a procedure was devised to estimate it. The core of the method was based on a graphical estimation of the point corresponding to the value of U_{Load}. To find the U_{Load} value an attempt was made that relied on finding the inflection point of the appropriate fragment of the curve depicting the relation of the voltage value to the time elapsed during the charge or discharge of the battery. Then an estimate was made using the said inflection point, so that the value of U_{Load} corresponding to that point could be read. This need originated from the fact that it was 'impossible' to use for this purpose the voltage value corresponding to the point labelled on Fig. 9(a) and 9(b) as $U_{LoadLast}$. The 'impossibility' resulted from the inherent meta-stability of the lead-acid galvanic cell. Since OCV requires stabilization and U_{OCV} was measured 15 minutes after the charge/load was disconnected (marked by the $U_{LoadLast}$ point), the state of the battery had since changed and the point that reflected the new state of the battery under load after the rest period---not before it---needed to be found.

The method described in [20] was used for the desulfation process. This method uses the following procedure (applied to the discharged battery): the battery is charged with a C/10 constant current for a period of 10 hours or until cell voltage reaches 2.4V per cell, followed by charging with constant voltage equal to 2.4 V per cell for 10 hours, with a final constant current charge with a current of C/50 for 50 hours. After that, discharge with C/10 is carried out to determine the amount of capacity regained. After these two steps another charge-discharge cycle follows, but this time the charging procedure consists of the first two charging steps mentioned above followed directly by the discharge step. According to [20] this procedure was repeated as many times as possible to regain at least 90% of the original capacity, then only the constant-current 10 hour C/10 rate charge and 14.4 V 10 hour constant-voltage are carried out until capacity reaches 100% of the battery's original capacity. For the purpose of the experiment reported in this paper, time constraints meant that the procedure was repeated only three times. The algorithm for the desulfation process is presented in Fig. 10. An exemplary graph showing the voltages and currents achieved during the desulfation cycle is presented in Fig. 11.

3. Results and discussion

To illustrate capacity loss over time, data was compiled in the form of graphs (see: Figs 12, 13, 14, 15 and 16). To calculate total capacity loss, the charge withdrawn from a battery in the last of all the discharge subcycles was divided by the nominal charge of 1.3 Ah and presented in graph form (Fig. 17).

The discharge and charge cycles originating data were analyzed and they led to interesting conclusions and observations. Batteries that were put in a buffer regime without any form of temperature compensation lost less capacity than expected. The assumption can be made here that the capacity loss possibly came from electrolyte loss rather than any other harmful process. Therefore, a later attempt to desulfate the batteries was used to confirm this and to determine whether the loss of capacity was due to reversible or irreversible processes.

The second pair of batteries where temperature compensation was used to reduce possible water loss suffered a large capacity loss. One of the batteries even suffered possible mechanical damage in one of the cells at the end of its eighth cycle, possibly due to electrode material destruction caused by aging-related sulfation. Intriguingly, and above all, the capacity loss in this particular case was not only bigger than in the first uncompensated pair, it was also bigger than in the fourth and fifth pairs, where temperature

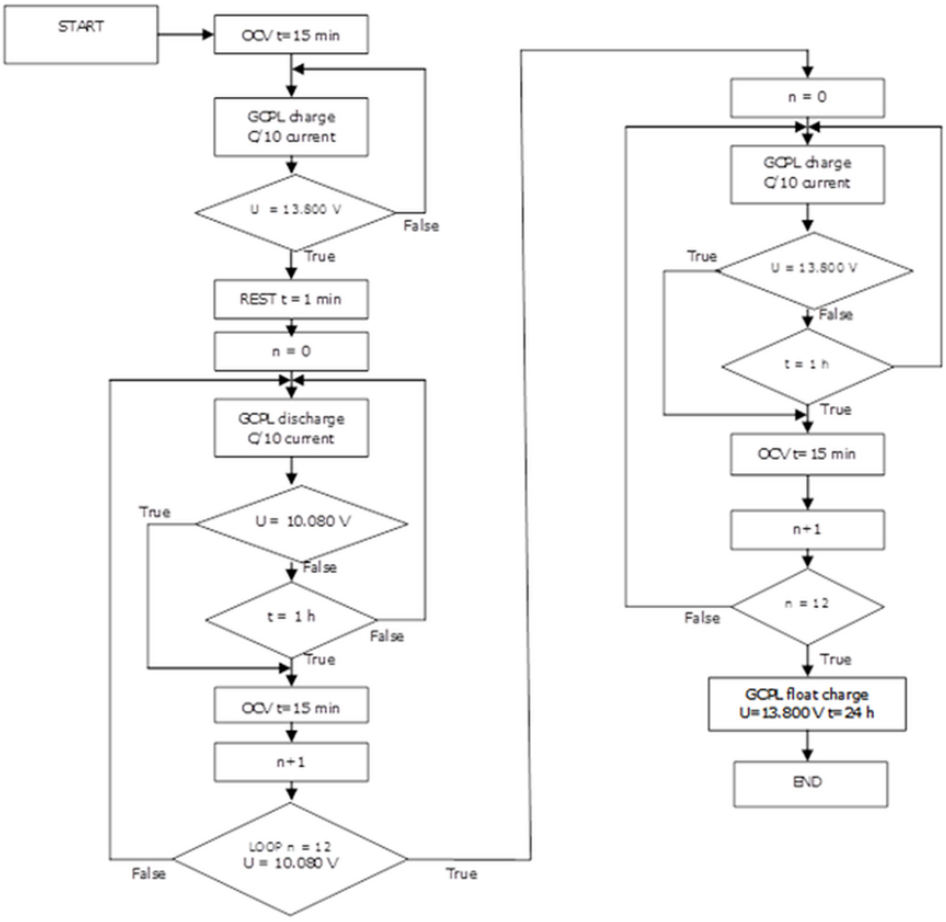

Figure 8: Algorithm for the aging experiment, including polarization resistance steps

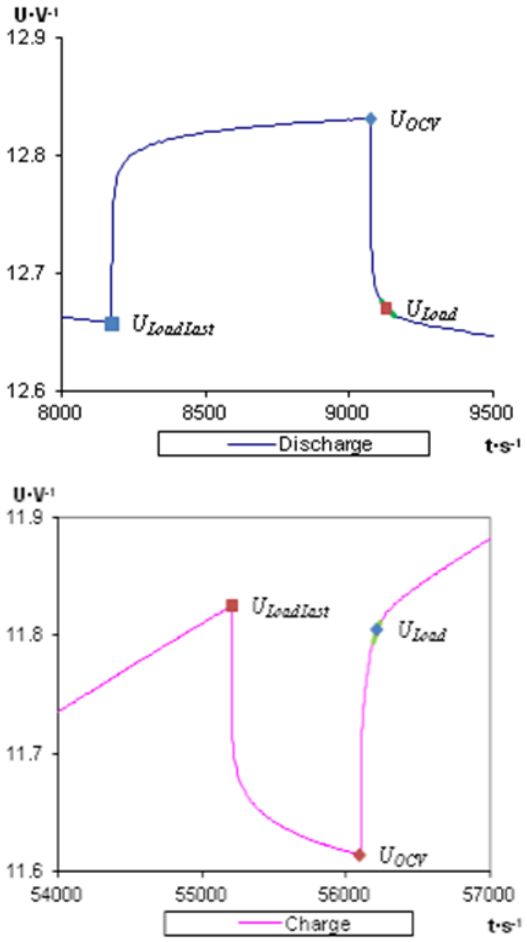

Figure 9: Finding the ULoad point for discharge sub-cycle - left and for the charge sub-cycle---right

compensated voltage was used in combination with simulated ripples. This runs contrary to reports that rippled float charging causes premature wearing of the battery due to the presence of harmful microcycles.

The third pair of batteries that was purposely sulfated suffered the largest and most rapid capacity loss, as predicted. This purposeful deterioration of battery performance was planned as a starting point for the later desulfation experiment, performed to determine whether any of that capacity could be regained.

The behavior of the fourth and fifth pairs was surprising, as both pairs exhibited less capacity loss than the second pair in all cycles, for all of the discharge rates. More surprisingly, the frequency and shape of the ripples had little impact on the capacity loss. It might be speculated that for both of these pairs the main aging process present in this situation was sulfation, as in the case of the second pair of batteries. The increased sulfation was most likely due to having a buffer voltage lower than 13.8V. It is also speculated that the lower capacity loss in the fourth and fifth pairs compared to the second pair of batteries might be attributed to the rippling having an impact that prevents sulfation. These assumptions are to be verified later.

Interestingly, three batteries suffered operational failure during the tests, which was registered during the 10th cycle. These were namely: battery 2 from the 2nd pair, battery 1 from the 3rd pair and battery 1 from the 4th pair. It was impossible to determine the exact cause of failure, but taking into consideration the charging regimes they were under, it can be speculated that the ensuing sulfation led to mechanical damage in the active material of the electrodes.

3.1. Polarization resistance investigation

While the investigation of the polarization resistance deviations for the battery discharge phase yielded no meaningful results, the same type of investigation conducted for the battery charging phase yielded a breakthrough in polarization resistance analysis. The results of the investigation suggested a new method for determining the gassing point. It was noted that batteries without temperature compensation exhibit a gassing point---the point where the harmful effect of the overcharge causes water decomposition [2, 4]. This gassing starts to affect the battery charging processes.

Determination of the gassing point is based on the observation that the battery's polarization resistance value exhibits an abrupt increase upon passing the gassing point. The R_{pol}=f(Q) dependence could be correlated with R_{pol}=f(U_{Charge}) dependence so a graphical method was devised to determine its value. The method requires a human operator to determine the initial and final slopes of the R_{pol}=f(Q) relation and to find the exact point where the slope changes. These two lines are shown on Fig. 18---one determined by the slope while only the charging process is present and the other characterized by the slope related to the occurrence of both the charging and the gassing processes; this makes it possible to find a value of Q corresponding to a gassing point. This value is correlated with the corresponding UCharge value, which is the final parameter that needs to be found.

Furthermore, it was tested if the other regimes exhibited the gassing point and it was determined that due to the lack of a sharp increase in battery polarization resistance, the gassing point cannot be observed.

3.2. Results and data analysis for the desulphation experiment

The primary objective of the desulfation procedure is to reduce the amount of active material that is trapped in the form of "hard sulfates" during battery operation. In turn this will result in the battery regaining some of its initially registered capacity. It should be noted that this desulfation procedure is to be performed late in the battery's life---as it aims to combat the sulfation resulting from long-term use rather than long-term storage. For batteries thoroughly sulfated due to long-term storage, without buffer voltage the said procedure would also apply; however, this is an issue which lies outside the remit of this paper.

To determine the success of the desulfation procedure, the data from the desulfation experiments was analyzed using

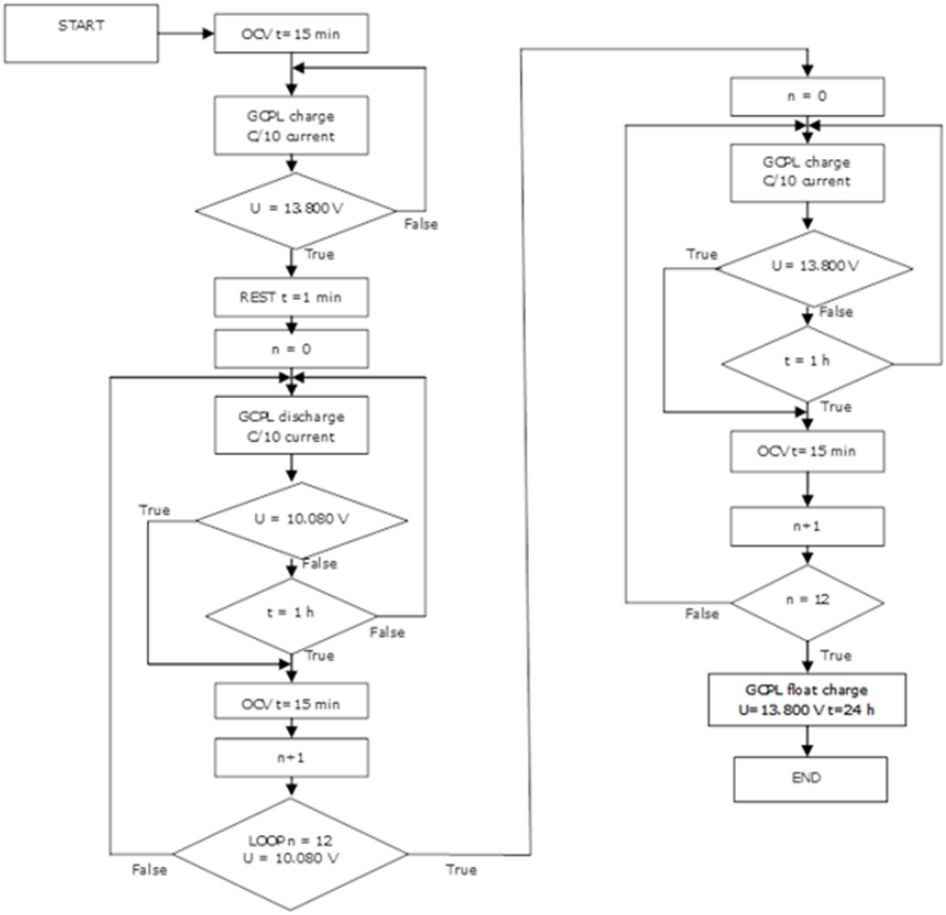

Figure 10: Algorithm for the desulfation experiment

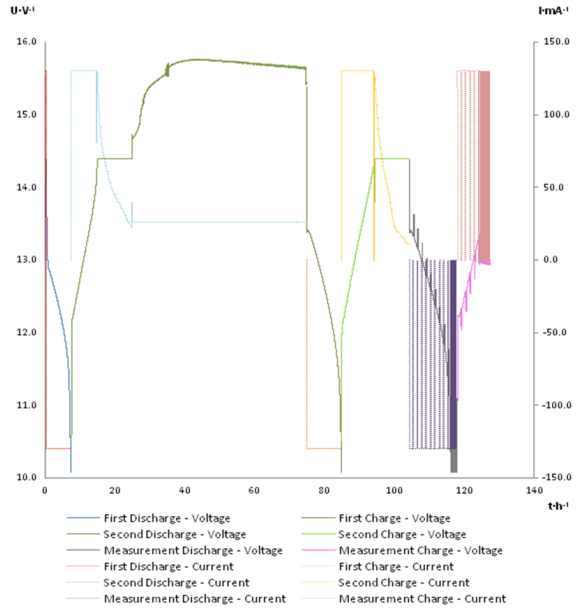

Figure 11: Exemplary voltage and current curves of a desulfation cycle

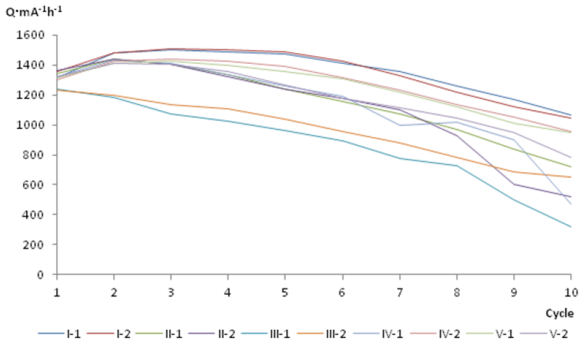

Figure 12: Changes of capacity in the batteries for discharge current of Q/10

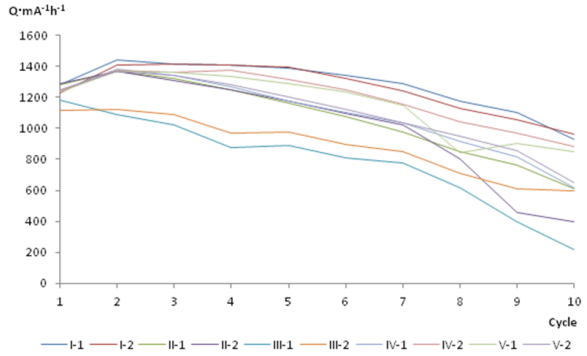

Figure 13: Changes of capacity in the batteries for discharge current of Q/5

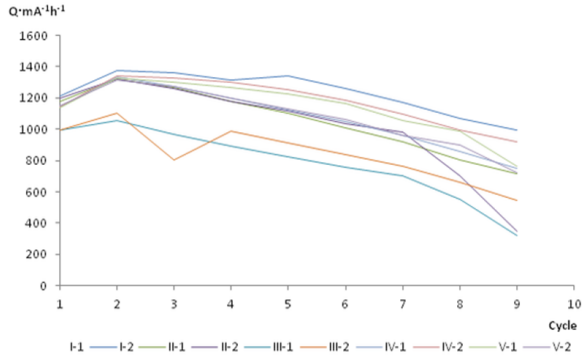

Figure 14: Changes of capacity in the batteries for discharge current of Q/3

two methods. The first method involved the following: As a measure of how much capacity was regained upon completion of the desulfation procedure, the charge delivered in the previously described post-desulfation test was compared with the charge delivered during the C/10 subcycle of the second cycle of the aging experiments. This was done to eliminate any possible error made due to overcharging. The second method used the comparison of the amount of charge taken out during C/10 discharge at the end of desulfation and at the end of the tenth cycle compared with the charge taken out during the C/10 subcycle of the second cycle of the aging experiment.

Two estimators were introduced to estimate the capacity regained by the procedure

$$E1 = \frac{Q_{10}}{Q_2} \cdot 100\% \tag{2}$$

– estimator determining the ratio between the total capacity that still remains in the battery after completion of the aging procedure and its capacity registered during the second discharge (referred to as 'initial discharge'). This estimator can provide information on the depth of deterioration that occurred during the battery aging process.

$$E2 = \frac{Q_{des}}{Q_2} \cdot 100\% \tag{3}$$

– estimator determining the ratio of the total capacity of battery after desulfation to the first registered capacity. This estimator can be used to determine the percentage of the nominal capacity of the battery achieved upon completion of the desulfation procedure. These estimators were used to determine the effectiveness of battery desulfation---the amount of capacity that was regained after the procedure has taken place. The previously described estimators will also help determine how much of the battery's active material is still 'trapped' in the non-active "hard sulfate" form [21]. The results of the set of experiments were compiled in graph form (Fig. 19 and 20).

A comparison of both efficency estimation methods shows that---other than the differences in the estimated values of battery capacity---there are differences in the qualitative outcome of the desulfation procedure. It was determined that the second method is the most accurate in the estimation of the desulfation procedure outcomes. Where irreversible capacity loss occurs due to gassing (first battery pair), the

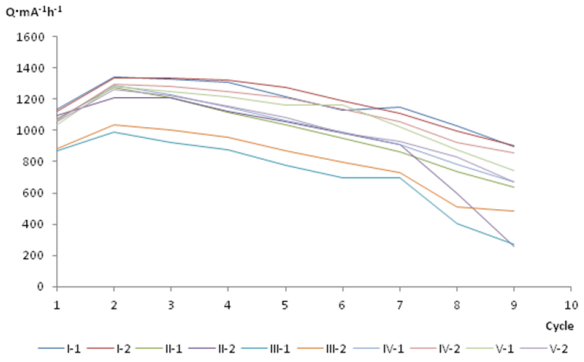

Figure 15: Changes of capacity in the batteries for discharge current of Q/2

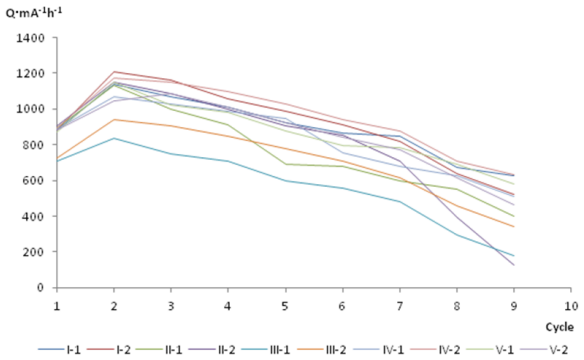

Figure 16: Changes of capacity in the batteries for discharge current of Q/1

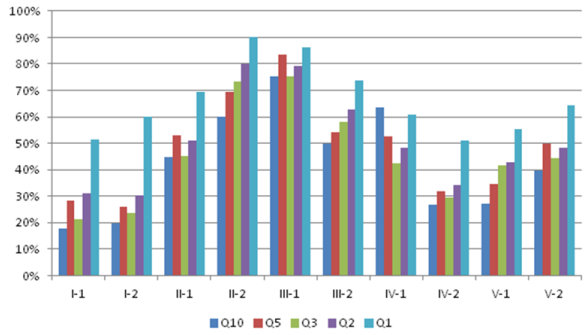

Figure 17: Percentage change of the battery's capacity for various discharge rates in relation to nominal charge

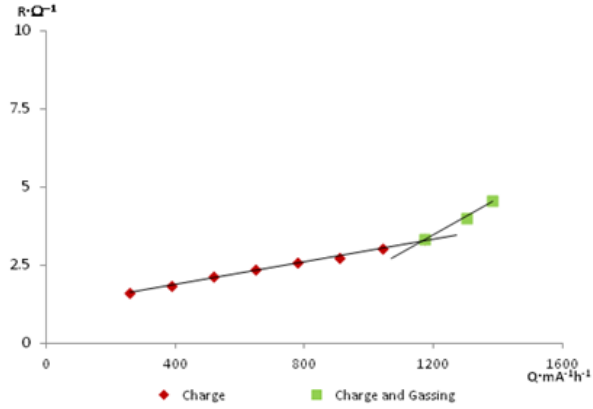

Figure 18: Example of determining a gassing point using a R_{pol}=f(Q) graph

first desulfation estimation method showed a rise in battery capacity after the procedure, where most likely it should not occur. And where desulfation should occur---for the 3rd battery pair, it shows that no such capacity regain was made. Thus this shows a great deal of inaccuracy in determining the qualitative outcome of the desulfation.

The batteries that were tested using rippling regimes (fourth and fifth pairs) and which had a smaller total capacity decrease were shown by the desulfation procedure to have a larger part of the capacity loss attributed to irrecoverable. This observation is made in comparison with the batteries tested using the non-rippled regime (second pair). The suggested explanation for this phenomenon is that rippling promotes 'quick' aging processes such as grid corrosion and gassing, in the periods of time when momentary voltage exceeds the average voltage value. On the other hand momentary under-voltage periods are too short to allow the sulfation to proceed significantly, as the recrystallization of lead sulfate is a rather slow process. Additionally, it may be that rippling might help break down large crystals of "hard sulfate" and thus free the active material trapped in this inert state of lead sulfate.

4. Results and discussion

It is already proven that the biggest impact on the battery life is the charging voltage. If it is too low, the sulphation processes can speed up considerably, rapidly decreasing battery lifetime. The rippling of the current seems to have lessen the speed of the processes as it is shown that capacity loss observed for the rippled currents is smaller compared to the unrippled current with temperature compensation. The nature of this phenomenon may lay in the fact that the fluctuating voltage and rate of charging current can prevent growth of large "hard sulphate crystals" and thus lead to lesser speed of sulphation. On the other hand desulpathion data for the same batteries, shows that the rippling might lead to the bigger irrecoverable capacity loss compared to that of the unrippled current. However more research is needed to determine the real nature of the observed phenomenon. The shape and the frequency of the ripples have smaller impact on the battery life. Testing has shown that the 12-pulse wave rippling causes a bit smaller battery degradation than the saw-tooth shaped wave.

The results of the battery desulphation prove to be interesting from few standpoints. The experiment proved to be a mild success as some lost capacity was regained in most cases, but it was not a complete capacity regain as it was

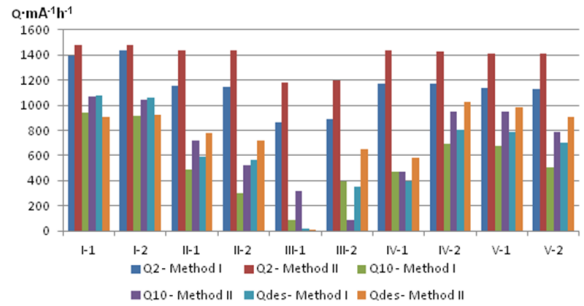

Figure 19: Percentage change of battery capacity for various discharge rates in relation to nominal charge

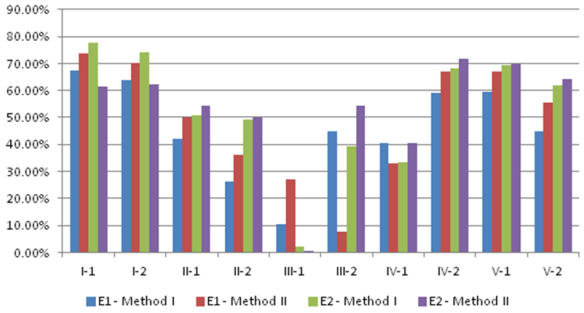

Figure 20: Comparison of estimators between two methods

hoped. A very interesting conclusion draws from this: it seems the ageing effects have a great impact on the batteries' ability to be desulphated. The best candidates for desulphation seemed to be the batteries that suffered smaller capacity losses as the bigger the capacity loss has been the bigger was the chance for the battery to not profit from this procedure. This is possible due to large "hard sulphate" crystal formations that not only block the sulphate that can be freed via electrode reactions, but also are unaffected by this desulphation regime.

One of the the major goals---to research whether the application of a sawtooth rippled current over the 12-pulse rippled current was less damaging to the batteries has succeed. The research conducted suggest that the impulse converters were not surpassing the thyristor-based ones in terms of reducing the damage to the battery. However, a bigger sample size may be needed to determine whether this observation is correct in all of the cases. It also has been shown that voltage reduction due to higher temperatures can lead to unwanted increase in sulphation rates. And lastly it also shown that proper desulphation regimes applied at right times can lead to capacity regain. The process used has been proven to show good result in batteries with capacity loss above 50%, but more investigation is needed to see whether it has any industrial usage.

Acknowledgments

This work was financially supported by The Faculty of Chemistry of Warsaw University of Technology

References

[1] C. Smith, Storage Batteries. Third Edition, Pitman Publishing Limited, London, 1980.
[2] D. Linden, B. Reddy, T, Handbook of Batteries. Third Edition, McGraw-Hill Professional, New York, 2002.
[3] G. Karlsson, Simple model for the overcharge reaction in valve regulated lead/acid batteries under fully stationary conditions, Journal of power sources 58 (1) (1996) 79–85.
[4] M. A. Karimi, H. Karami, M. Mahdipour, Ann modeling of water consumption in the lead-acid batteries, Journal of Power Sources 172 (2) (2007) 946–956.
[5] S. Bai, S. Lukic, A 12-pulse diode rectifier with energy storage integration and high power quality on both ac and dc side, in: Energy Conversion Congress and Exposition (ECCE), 2012 IEEE, IEEE, 2012, pp. 4042–4048.
[6] Materials from www.eurobat.org.
[7] Y. B. Blauth, I. Barbi, A phase-controlled 12-pulse rectifier with unity displacement factor without phase shifting transformer, in: Applied Power Electronics Conference and Exposition, 1998. APEC'98. Conference Proceedings 1998., Thirteenth Annual, Vol. 2, IEEE, 1998, pp. 970–976.
[8] A. Ruddell, A. Dutton, H. Wenzl, C. Ropeter, D. Sauer, J. Merten, C. Orfanogiannis, J. Twidell, P. Vezin, Analysis of battery current microcycles in autonomous renewable energy systems, Journal of Power sources 112 (2) (2002) 531–546.
[9] C. Protogeropoulos, J. Nikoletatos, "EXAMINATION OF RIPPLE CURRENT EFFECTS ON LEAD-ACID BATTERY AGEING AND TECHNICAL AND ECONOMICAL COMPARISON BETWEEN "SOLAR" AND SLI BATTERIES", 14th EC Photovoltaic Solar Energy Conference, Barcelona, Spain, 1997.
[10] R. F. Nelson, M. A. Kepros, Ac ripple effects on vrla batteries in float applications, in: Battery Conference on Applications and Advances, 1999. The Fourteenth Annual, IEEE, 1999, pp. 281–289.
[11] P. T. Moseley, J. Garche, Electrochemical energy storage for renewable sources and grid balancing, Newnes, 2014.
[12] D. U. Sauer, H. Wenzl, Comparison of different approaches for lifetime prediction of electrochemical systems—using lead-acid batteries as example, Journal of Power sources 176 (2) (2008) 534–546.
[13] L. Lam, N. Haigh, C. Phyland, A. Urban, Failure mode of valve-regulated lead-acid batteries under high-rate partial-state-of-charge operation, Journal of Power Sources 133 (1) (2004) 126–134.
[14] B. Zhang, J. Zhong, W. Li, Z. Dai, Z. Cheng, Transformation of inert pbso4 deposit on the negative electrode of a lead-acid battery into its active state, Journal of Power Sources 195 (13) (2010) 4338–4343.
[15] D. Pavlov, G. Petkova, T. Rogachev, Influence of h2so4 concentration on the performance of lead-acid battery negative plates, Journal of Power Sources 175 (1) (2008) 586–594.
[16] L. Lam, H. Ceylan, N. Haigh, T. Lwin, D. Rand, Influence of residual elements in lead on oxygen-and hydrogen-gassing rates of lead-acid batteries, Journal of Power Sources 195 (14) (2010) 4494–4512.
[17] L. Lam, O. Lim, N. Haigh, D. Rand, J. Manders, D. Rice, Oxide for valve-regulated lead–acid batteries, Journal of power sources 73 (1) (1998) 36–46.
[18] M. Saravanan, S. Ambalavanan, Failure analysis of cast-on-strap in lead-acid battery subjected to vibration, Engineering Failure Analysis 18 (8) (2011) 2240–2249.
[19] T. Khun, The Electrochemistry of Lead, Academic Press, London, 1979.
[20] D. U. Sauer, E. Karden, B. Fricke, H. Blanke, M. Thele, O. Bohlen, J. Schiffer, J. B. Gerschler, R. Kaiser, Charging performance of automotive batteries—an underestimated factor influencing lifetime and reliable battery operation, Journal of power sources 168 (1) (2007) 22–30.
[21] M. Thele, J. Schiffer, E. Karden, E. Surewaard, D. Sauer, Modeling of the charge acceptance of lead–acid batteries, Journal of Power Sources 168 (1) (2007) 31–39.